Alcohol 48 (2014) 707–715

Contents lists available at ScienceDirect

Alcohol

journal homepage: http://www.alcoholjournal.org/

Dietary umbelliferone attenuates alcohol-induced fatty liver via regulation of PPARα and SREBP-1c in rats

Myung-Joo Kim [a,1], Mi-Ok Sim [b,1], Hae-In Lee [c], Ju Ri Ham [c], Kwon-Il Seo [c], Mi-Kyung Lee [c,*]

[a] Department of Hotel Cuisine, Suseong College, Daegu, 706-022, Republic of Korea
[b] Jeollanamdo Development Institute of Korean Traditional Medicine, Jangheung, 529-851, Republic of Korea
[c] Department of Food and Nutrition, Sunchon National University, 255 Jungang-ro, Suncheon, Jeonnam, 540-950, Republic of Korea

Keywords:
Alcoholic fatty liver
Lipid metabolism
SREBP-1c
PPARα
Umbelliferone

A B S T R A C T

This study investigated the effects of umbelliferone (UF) on alcoholic fatty liver and its underlying mechanism. Rats were fed a Lieber–DeCarli liquid diet with 36% of calories as alcohol with or without UF (0.05 g/L) for 8 weeks. Pair-fed rats received an isocaloric carbohydrate liquid diet. UF significantly reduced the severity of alcohol-induced body weight loss, hepatic lipid accumulation and droplet formation, and dyslipidemia. UF decreased plasma AST, ALT, and γGTP activity. UF significantly reduced hepatic cytochrome P450 2E1 activities and increased alcohol dehydrogenase and aldehyde dehydrogenase 2 activities compared to the alcohol control group, which resulted in a lower plasma acetaldehyde level in the rats that received UF. Chronic alcohol exposure inhibited hepatic AMPK activation compared to the pair-fed rats, which was reversed by UF supplementation. UF also significantly suppressed the lipogenic gene expression (SREBP-1c, SREBP-2, FAS, CIDEA, and PPARγ) and elevated the fatty acid oxidation gene expression (PPARα, Acsl1, CPT, Acox, and Acaa1a) compared to the alcohol control group, which could lead to inhibition of FAS activity and stimulation of CPT and fatty acid β-oxidation activities in the liver of chronic alcohol-fed rats. These results indicated that UF attenuated alcoholic steatosis through down-regulation of SREBP-1c-mediated lipogenesis and up-regulation of PPARα-mediated fatty acid oxidation. Therefore, UF may provide a promising natural therapeutic strategy against alcoholic fatty liver.

Introduction

Alcoholic liver disease is associated with excessive alcohol consumption and is a major cause of mortality and morbidity worldwide. Fatty liver is the most frequent primary change in chronic alcohol abuse, leading to more severe forms of liver injury, including alcoholic hepatitis, cirrhosis, and hepatocellular carcinoma. Over 90% of heavy drinkers develop fatty liver and 10–35% of those develop hepatitis. About 8–20% of chronic alcoholics develop liver cirrhosis, which may eventually lead to hepatocellular carcinoma (WHO, 2011).

Fatty liver is characterized by the accumulation of fat primarily in the form of triglycerides, phospholipids, and cholesterol esters in hepatocytes (Gao & Bataller, 2011). Recent studies have indicated that alcohol may regulate lipid metabolism-related transcription factors, resulting in stimulation of lipogenesis and inhibition of fatty acid oxidation (Rasineni & Casey, 2012). Alcohol consumption could directly increase sterol regulatory element binding transcription factor 1c (SREBP-1c) gene expression via its metabolite acetaldehyde, and inhibit fatty acid oxidation via inactivation of the peroxisome proliferator-activated receptor alpha (PPARα), a nuclear hormone receptor that controls transcription of genes involved in free fatty acid transport and oxidation (Gao & Bataller, 2011). Therefore, SREBP-1c and PPARα are attractive targets for treatment or prevention of alcoholic fatty liver diseases.

Umbelliferone (UF) (Fig. 1) is a coumarin derivative present in fruits and plants, such as *Angelica decursiva, Artemisia capillaris*, golden apple, and bitter orange (Jung et al., 2012; Kanimozhi, Prasad, Ramachandran, & Pugalendi, 2011; Zhao et al., 2012). The antinociceptive effect of UF has been shown to be correlated with inhibition of cytokine release and prostaglandin E_2 (de Lima et al., 2011). Kanimozhi et al. (2011) demonstrated that UF exhibits radioprotective abilities by free radical scavenging, inhibiting radiation-induced DNA damage, and increasing the antioxidant status and antiperoxidative potential in human peripheral blood lymphocytes. Li and Ellis (2012) suggested that UF (100 μM) was able to increase the expression of aldo-keto reductases in human astrocytoma 1321N1 cells, which was associated with enhanced ability to detoxify reactive aldehydes. Ramesh and Pugalendi

Conflict of interest: The authors have no conflicts of interest to declare.

* Corresponding author. Tel.: +82 61 750 3656; fax: +82 61 752 3657.
E-mail address: leemk@sunchon.ac.kr (M.-K. Lee).

[1] These authors contributed equally to this work.

0741-8329/$ – see front matter © 2014 Elsevier Inc. All rights reserved.
http://dx.doi.org/10.1016/j.alcohol.2014.08.008

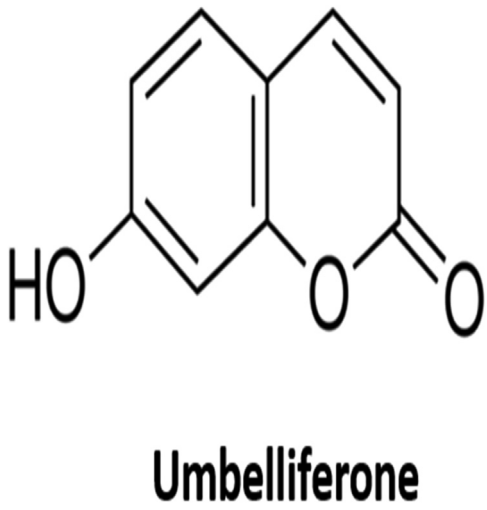

Fig. 1. Chemical structure of UF.

(2006a, 2006b) reported that UF has significant glucose reducing and antioxidant properties, as demonstrated by decreased gluconeogenic enzymes and lipid peroxidation. Our previous study showed that UF might protect against high-fat diet-induced hepatic lipid accumulation in mice (Sim, Ham, Lee, Seo, & Lee, 2014). However, protective action of UF against alcoholic fatty liver has not been investigated. Therefore, this study was conducted to investigate the effects of UF on alcoholic fatty liver in rats through hepatic lipid metabolic gene expressions.

Materials and methods

Animals and diets

Twenty-four male Sprague–Dawley rats (4 weeks old) were purchased from Orient Bio Inc. (Seoul, Korea). After a 1-week adaptation period, the animals were randomly divided into a pair-fed group, alcohol control group, and UF (0.05 g/L diet, Sigma, St. Louis, MO, USA) supplemented with alcohol diet group. The dose of UF used was based on our previous study as well as other studies that have investigated the protective effects of UF on hepatotoxicity (Sim et al., 2014; Stefanova, Nikolova, Michailova, et al., 2007; Stefanova, Nikolova, Toshkova, & Neychev, 2007). The animals were individually housed in stainless-steel cages in an air-conditioned room with a controlled temperature (20 ± 2 °C), humidity (50 ± 5%), and light cycle (alternating 12-h periods of light and dark) for 8 weeks. The rats in the alcohol groups were given a liquid alcohol diet (36% of calories) in which ethanol was introduced progressively in increasing concentrations. Specifically, animals were provided with 3% ethanol for the first 2 days (21% of total calories), 4% for the next 2 days (28% of calories) and 5% (36% of calories) thereafter (Lieber & DeCarli, 1989). The pair-fed rats received an isocaloric liquid diet containing dextrin-maltose instead of ethanol (Table S1). The rats in the alcohol and UF groups received food *ad libitum*, while the pair-fed animals received the same amount of diet that the alcohol control rats consumed the previous day. Body weight and food intake were measured once a week and daily, respectively. The present study was approved by the Sunchon National University Institutional Animal Care and Use Committee.

At the end of the experimental period, the animals were anesthetized with CO_2 gas following a 12-h fast. Blood was then drawn from the inferior vena cava into a tube with heparin coating. Plasma was obtained by centrifuging the blood at 900×*g* for 15 min at 4 °C. The organs were then removed, rinsed with physiological saline, and immediately weighed. The plasma and organ samples were stored at −70 °C until analysis.

Plasma liver damage biomarkers

To assess liver damage, the plasma aspartate aminotransferase (AST), alanine aminotransferase (ALT), and gamma glutamyl transpeptidase (γGTP) activities were measured using an automated chemistry analyzer (Fuji-Dri-Chem 3500; Fujifilm, Tokyo, Japan).

Plasma and hepatic lipid levels

The plasma total cholesterol, HDL-cholesterol, triglyceride (Asan Diagnostics, Seoul, Korea), and free fatty acid (Shinyang Diagnostics, Seoul, Korea) concentrations were determined using commercial kits. The hepatic lipid was extracted as previously described (Do et al., 2011), after which the cholesterol and triglyceride contents were analyzed using the same enzymatic kit that was used for the plasma analysis.

Hepatic histological analysis

The liver was removed and fixed in a buffer solution containing 10% formalin, after which the fixed tissues were paraffin-embedded, and 3–5-μm sections were prepared and stained with hematoxylin and eosin. The stained area was viewed using a microscope at a magnification of 200×.

Plasma acetaldehyde levels and alcohol metabolic enzyme activities

The plasma acetaldehyde (R-Biopharm, Roche, Darmstadt, Germany) levels were determined using an enzymatic bioassay. Briefly, acetaldehyde was quantitatively oxidized to acetic acid in the presence of aldehyde dehydrogenase and nicotinamide adenine dinucleotide (NAD). The amount of NADH formed was stoichiometric to the amount of acetaldehyde. The activities of alcohol dehydrogenase (ADH) and aldehyde dehydrogenase 2 (ALDH2) were assayed in the liver as previously described (Lee et al., 2013). The conversion of NAD^+ to NADH was observed by recording the changes in absorbance at 340 nm for 5 min after the initiation of the enzyme reaction. The hepatic microsomal cytochrome P450 2E1 (CYP2E1) activity was determined by measuring the formation of 4-nitrocatechol (Lee et al., 2013).

RNA isolation and quantitative real-time PCR analysis

The liver was homogenized in Trizol reagent (Invitrogen Life Technologies, Grand Island, NY, USA), after which total RNA was isolated according to the manufacturer's specifications. DNase digestion was used to remove any DNA contamination, after which the RNA was re-precipitated in ethanol to ensure that there was no phenol contamination. For quality control, RNA purity and integrity were evaluated using an Agilent 2100 Bioanalyzer (Agilent Technologies, Palo Alto, USA). The total RNA (1 μg) was reverse-transcribed into cDNA using a QuantiTect® reverse transcription kit (Qiagen, Hilden, Germany). Next, mRNA expression was quantified by real-time quantitative PCR using an SYBR green PCR kit (Qiagen, Hilden, Germany) and the CFX96TM real-time system (Bio-Rad, Hercules, CA, USA). The sequences of the primers were shown in supplementary data (Table S2). The cycle thresholds were determined based on the SYBR green emission intensity during the exponential phase. The fold changes were determined using the $2^{\triangle\triangle Ct}$ method (Livak & Schmittgen, 2001). In addition,